



HAL
open science

Correction to Vibro-Polaritonic IR Emission in the Strong Coupling Regime

Marcus Seidel, Thibault Chervy, Anoop Thomas, Elias Akiki, Robrecht Vergauwe, Atef Shalabney, Jino George, Eloise Devaux, James A Hutchison, Cyriaque Genet, et al.

► **To cite this version:**

Marcus Seidel, Thibault Chervy, Anoop Thomas, Elias Akiki, Robrecht Vergauwe, et al.. Correction to Vibro-Polaritonic IR Emission in the Strong Coupling Regime. *ACS photonics*, 2019, 6 (7), pp.1823-1825. 10.1021/acsp Photonics.8b01756 . hal-03115959

HAL Id: hal-03115959

<https://hal.science/hal-03115959v1>

Submitted on 19 Jan 2021

HAL is a multi-disciplinary open access archive for the deposit and dissemination of scientific research documents, whether they are published or not. The documents may come from teaching and research institutions in France or abroad, or from public or private research centers.

L'archive ouverte pluridisciplinaire **HAL**, est destinée au dépôt et à la diffusion de documents scientifiques de niveau recherche, publiés ou non, émanant des établissements d'enseignement et de recherche français ou étrangers, des laboratoires publics ou privés.

Correction to Vibro-Polaritonic IR Emission in the Strong Coupling Regime

Marcus Seidel,[†] Thibault Chervy,^{†,¶} Anoop Thomas,[†] Elias Akiki,[†] Robrecht M. A. Vergauwe,[†] Atef Shalabney,[‡] Jino George,[†] Eloïse Devaux,[†] James A. Hutchison,[†] Cyriaque Genet,[†] and Thomas W. Ebbesen^{*,†}

[†]*ISIS & icFRC, University of Strasbourg, CNRS, 8 Allée Gaspard Monge, 67000
Strasbourg, France*

[‡]*Braude College, Snunit Street 51, Karmiel 2161002, Israel*

[¶]*Current address: Department of Physics, ETH Zurich, Switzerland*

E-mail: ebbesen@unistra.fr

Phone: +33 (0) 3 68 85 51 16

Abstract

ACS Photonics **2018**, 5 (1), 217-224. DOI: 10.1021/acsp Photonics.7b00677

The method of fitting the micro-cavity transmission spectrum to derive the cavity absorption spectrum by means of transfer matrix analysis was flawed. Consequently, by contrast to our initial conclusions, the polaritonic emission appears thermalized and there is no evidence for polariton emission which is blue-shifted with respect to the polariton absorption. For this reason, the interpretation of the blue-shift as a signature of polariton-polariton interactions is obsolete.

Two errors have been made: First, the dielectric function of PMMA was only modeled in the range from 1400 cm^{-1} to 2100 cm^{-1} (original Figure 2 (b)). However, by virtue of

the Kramers-Kronig relations, the relatively strong absorption lines at lower energies (cf. original Figure 2(a)) influence the refractive index in the vicinity of the strongly coupled C=O stretching band. Therefore, the simulated free spectral ranges between the cavity and the polariton modes were incorrect. Second, a small aperture was kept inside the Fourier transform infrared (FTIR) spectrometer transmission compartment for both emission and transmission measurements. As a consequence, only a small area of the prepared cavity was sampled. It was not checked which part of the emitting sample was imaged onto the aperture in the transmission compartment. Therefore, it is likely that different spots of the same sample were measured in transmission and emission, respectively. A film thickness inhomogeneity on the order of 10 nm (the polymer film was about $4\ \mu\text{m}$ thick) can cause a spectral shift of the modes on the order of the initially derived polariton blue-shift ($17\ \text{cm}^{-1}$ and $6\ \text{cm}^{-1}$). Both errors added up in a way that the transmission spectrum fit yielded a match of emission maxima and reflectivity minima at the 1st and the 3rd cavity mode, as expected from thermalized emission (cf. original Figure 3 (b)). The emission maxima appeared however blue-shifted with respect to the reflection minima (cf. original Figure 3 (d)). It is to note that absorption maxima and reflection minima overlap.

In an analogous manner to the procedure described in the original paper, we spin-coated an about $1\ \mu\text{m}$ thick PMMA film on a 0.5 mm thick silicon substrate. We measured the sample transmission with an FTIR spectrometer and fitted it by transfer matrix analysis while optimizing the model of the dielectric function of PMMA. The silicon substrate was treated as an incoherent layer. Its complex refractive index was taken from the literature¹ and was in good agreement with experimental data. To approximate the dielectric function of PMMA, we started from the Lorentz-oscillator model used in the original paper. Next, we adjusted the imaginary part of the PMMA complex refractive index and finally applied Kramers-Kronig relations to obtain the real part of the refractive index.² Figure 1 shows the measured transmission spectrum, the fit with the originally used simplified dielectric function and the fit with the refined dielectric function.

Consequently, we fitted again the cavity transmission and emission data originally published. The fit of the polaritonic transmission peaks is shown in Figure 2(a). The horizontal black bar denotes the spectral region which has previously been considered (original Figure 2(b)). Subsequently, the polaritonic peaks are modeled well by both dielectric functions. However, the transmission peaks of the 1st and the 3rd cavity mode are only well matched by the refined dielectric function whereas the simulation predicts blue-shifted peaks for the originally used function. Figure 2(b) shows the derived normalized absorption spectra and compares them to the experimentally determined emissivity. The use of the original dielectric function results in a good agreement between the 1st and the 3rd cavity mode peak locations, but a larger discrepancy between the measured and simulated lower polariton emissivity peaks. This led to the original conclusion of non-thermal polariton emission. By contrast, the refined dielectric function shows not only a spectral offset for the polariton peaks, but also for the peaks of the bare cavity modes, that is, the whole simulated absorption spec-

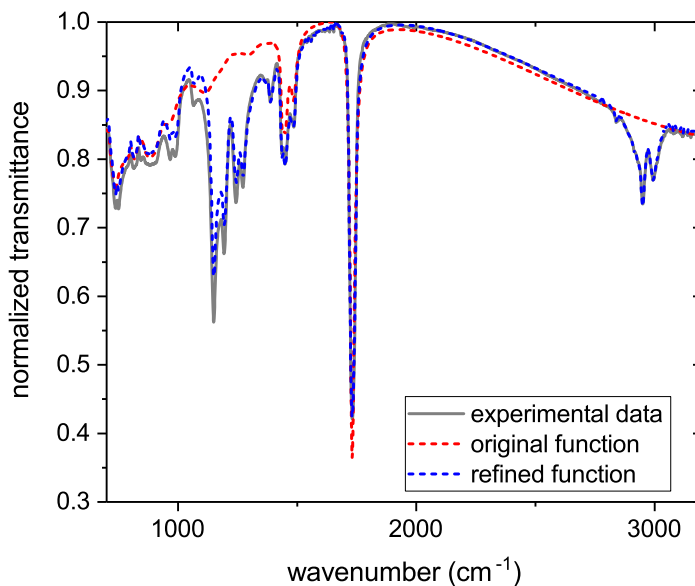


Figure 1: Modeling of the PMMA dielectric function. Gray solid line: normalized transmittance spectrum of a $1.05\ \mu\text{m}$ PMMA film on a Si substrate measured with a FTIR spectrometer. Red dashed line: Model of the dielectric function used in the original paper. Blue dashed line: refined model of the dielectric function including more absorption lines.

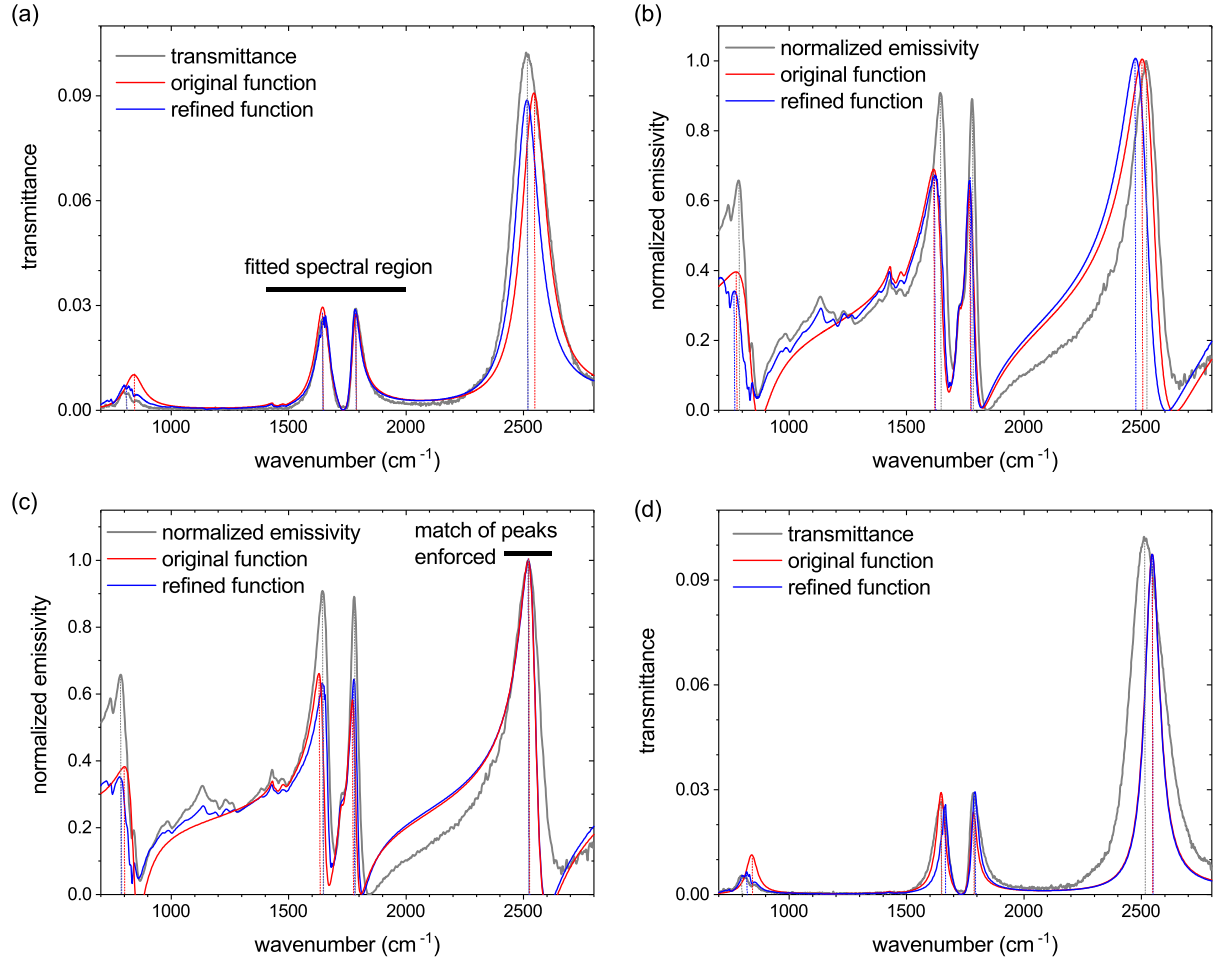


Figure 2: Modeling the original data by transfer-matrix simulations. **(a)** The measured transmittance is fitted in the spectral region marked by the black bar (cf. original Figure 2(b)). **(b)** From the transmittance fit, the cavity absorption is derived by the transfer-matrix approach. According to Kirchhoff’s law, it should correspond to the cavity emissivity. **(c)** The measured emissivity peak of the 3rd cavity mode is matched with the simulated absorption peaks. **(d)** The transmittance corresponding to the absorption in (c) is derived and compared to the original data. The solid gray lines represent the original data, the solid red lines the simulations by means of the original dielectric function and the solid blue lines the simulations by means of the refined dielectric function. The emissivity plots have been normalized to simplify comparison of data and simulations. The vertical dashed lines show the peak locations.

trum is red-shifted with respect to the experimentally determined emissivity spectrum. In Figure 2(c), this shift is corrected by enforcing the overlap of the 3rd cavity mode absorption and emissivity peaks. This results in excellent agreement between the emissivity peaks and the absorption peaks modeled with the refined dielectric function. The original dielectric

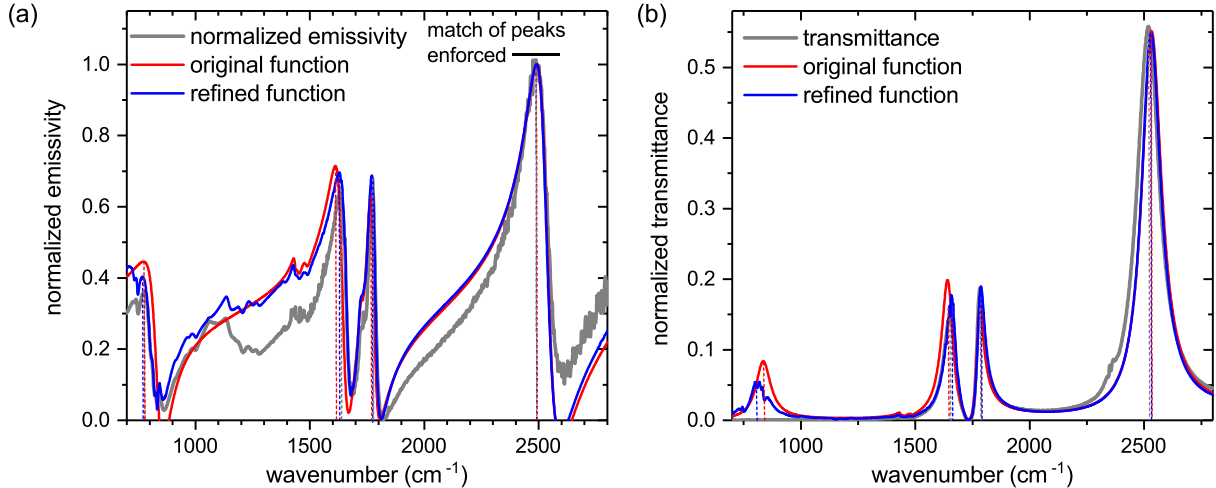


Figure 3: Experimental data and transfer-matrix analysis of a second strongly-coupled microcavity. **(a)** Like in Figure 2(c), the measured emissivity peak of the 3rd cavity mode is matched with the simulated absorption peaks. **(b)** Like in Figure 2(d), the transmittance corresponding to the absorption in (a) is derived and compared to the experimental data. The experimental transmittance at the 1st cavity mode is 0 due to the ZnS absorption. The substrate absorption was not taken into account in the transfer-matrix analysis.

function, however, shows offsets between absorption and emissivity peaks of the 1st cavity mode as well as the polaritons. Finally, the corresponding transmission spectra are shown in Figure 2(d). They are computed by means of the cavity parameters used in Figure 2(c). The clear offsets between experimental and simulated 3rd cavity mode peaks manifest that the originally measured transmittance and emissivity spectra were not directly comparable as the locally sampled cavity lengths were different.

To attain consistence between simulations, emissivity and transmittance measurements, we prepared another Fabry-Pérot cavity comparable to the one used to collect the original data. We used a ZnS substrate, sputter-coated an about 10 nm thin Au film on it, spin-coated an about 4 μm thick PMMA layer on top and finally closed the cavity by sputter-coating another about 10 nm thin Au film. We removed the aperture from the transmission compartment of the FTIR to sample the same cavity area in emission and transmission. As a consequence, the signal-to-noise-ratio in the emission measurement was reduced, and thus we performed an additional correction for atmospheric absorptions in the FTIR and

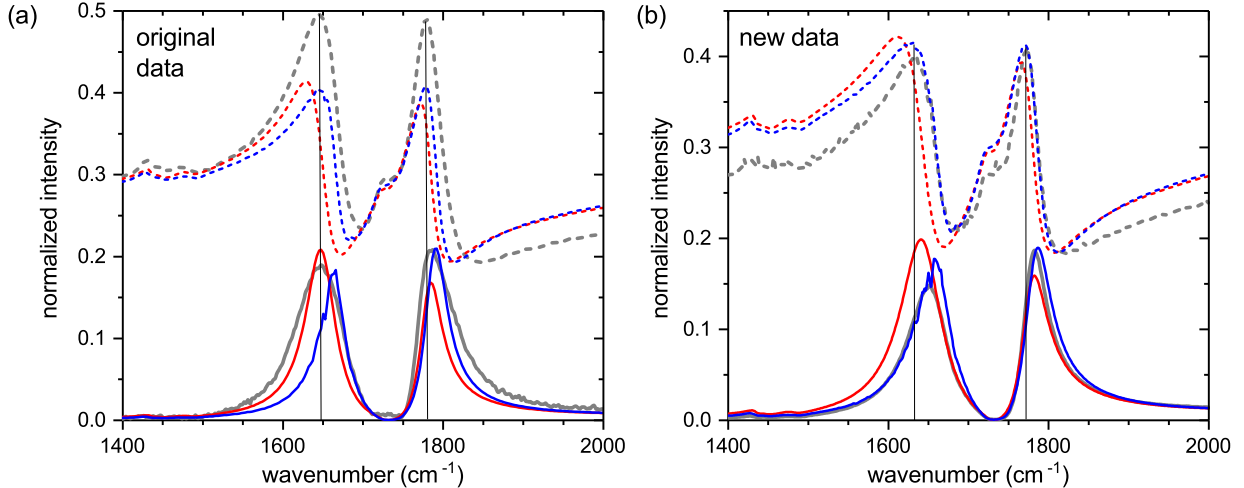


Figure 4: Transmittance and emissivity in the spectral range from 1400 cm^{-1} to 2000 cm^{-1} for **(a)** the original data (cf. Figure 2) and **(b)** the recently acquired data (cf. Figure 3). Solid lines represent transmittance spectra, dashed lines emissivity spectra, gray lines experimental data, red lines transfer-matrix simulations with the initially used dielectric function of PMMA and blue lines transfer-matrix simulations with the refined dielectric function.

we subtracted the reference spectrum from the signal of the sample and the experimental blackbody spectrum (cf. Eq. (13) of the original paper). Measurement results and simulations are shown in Figure 3. As in Figure 2(c) and (d), the peaks of 3rd cavity mode emissivity and simulated absorption were matched. Figure 3(a) exhibits again an overlap of simulated and measured polariton emission peaks if the refined dielectric function is used, whereas the original dielectric function predicts blue-shifted emission of the lower polariton. This is highlighted in Figure 4 where only the spectral range from 1400 cm^{-1} to 2000 cm^{-1} is considered like in Figure 3(d) of the original publication. The absence of the aperture in the transmission compartment leads to a clearly improved agreement between measured and simulated transmittance spectra as the comparison between the Figures 2(d) and 3(b) demonstrates. The shift between measured and simulated 3rd cavity mode as well as the linewidth difference is much smaller in the latter case. The refined dielectric function leads also to a good agreement between measured and simulated transmittance of the polariton modes as Figure 4(b) shows.

In addition to the funding acknowledged in the original publication, M.S. acknowledges

support from the Marie Skłodowska-Curie actions of the European Commission (project 753228, PlaN).

References

- (1) Chandler-Horowitz, D.; Amirtharaj, P. M. High-accuracy, midinfrared ($450 \text{ cm}^{-1} \leq \omega \leq 4000 \text{ cm}^{-1}$) refractive index values of silicon. *Journal of Applied Physics* **2005**, *97*, 123526.
- (2) Törmä, P.; Barnes, W. L. Strong coupling between surface plasmon polaritons and emitters: a review. *Reports on Progress in Physics* **2015**, *78*, 013901.